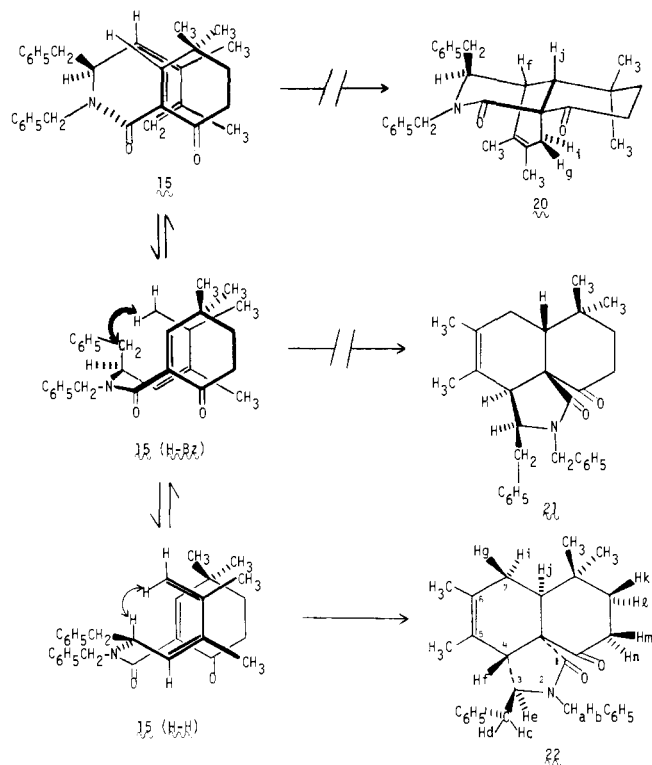


## Scheme II



that under identical conditions the isomeric *E*-amide **19** (Scheme I) is recovered largely unchanged. The structure of lactam **22**, although firmly supported by spectral analysis,<sup>15,23</sup> was additionally verified by X-ray analysis (Figure 1).<sup>24</sup> This finding indicates that cyclization has occurred specifically via the indicated **15** (H-H) transition state<sup>25</sup> with the exclusion of alternate products **20** and **21** (Scheme II).

**Acknowledgments.** We thank the National Science Foundation (CHE 79-03953) and the National Institute of Health (AI-13073) for their generous support of this work. The carbon-13 NMR data reported in this investigation were obtained on the departmental CFT-20 instrument provided by NSF Grant 7842. We thank Preston Conrad for providing those spectra. We also thank the Purdue University Biological Magnetic Resonance Laboratory (NIH RR01077) for access to the 360-MHz <sup>1</sup>H NMR spec-

(23) For **22** atoms have been numbered according to the cytochalasin numbering system:  $\nu_{\max}$  (CHCl<sub>3</sub>) 5.88, 5.95  $\mu\text{m}$ ; <sup>1</sup>H NMR (360 MHz, CDCl<sub>3</sub>)  $\delta$  7.25-7.10 (m, 10 H, aryl), 5.17 (d,  $J_{ab} = 15.4$  Hz, H<sub>a</sub>), 3.91 (d,  $J_{ab} = 15.4$  Hz, H<sub>b</sub>), 3.20 (dd,  $J_{ce} = 5.3$  Hz,  $J_{de} = 9.8$  Hz,  $J_{ef} < 1$  Hz, H<sub>e</sub>), 3.05 (dd,  $J_{ce} = 5.3$  Hz,  $J_{od} = 13.2$  Hz, H<sub>c</sub>), 2.81 (ddd,  $J_{mn} = J_{kn} = 14.2$  Hz,  $J_{ln} = 5.8$  Hz, H<sub>n</sub>), 2.51 (d,  $J_{gi} = 6.4$  Hz, H<sub>j</sub>), 2.50 (dd,  $J_{od} = 13.2$  Hz,  $J_{de} = 9.8$  Hz, H<sub>d</sub>), 2.45 (ddd,  $J_{mn} = 14.2$  Hz,  $J_{km} = 4.0$  Hz,  $J_{lm} = 4.5$  Hz, H<sub>m</sub>), 2.39 (br s,  $J_{ef} < 1$  Hz, H<sub>f</sub>), 2.11 (ddq,  $J_{gi} = 17.5$  Hz,  $J_{ji} = 6.4$  Hz,  $J_{CH_3(S)g} = 1.5$  Hz, H<sub>g</sub>), 1.89 (d,  $J_{ji} = 17.5$  Hz, H<sub>i</sub>), 1.88 (ddd,  $J_{kl} = 15.5$  Hz,  $J_{km} = 4.0$  Hz,  $J_{kn} = 14.2$  Hz, H<sub>k</sub>), 1.74 (ddd,  $J_{kl} = 15.5$  Hz,  $J_{lm} = 4.5$  Hz,  $J_{ln} = 5.8$  Hz, H<sub>l</sub>), 1.55 (brs, C<sub>6</sub>-CH<sub>3</sub>), 1.05 (s, CH<sub>3</sub>), 0.90 (d,  $J_{CH_3(S)g} = 1.5$  Hz C<sub>5</sub>-CH<sub>3</sub>), 0.82 (s, CH<sub>3</sub>); <sup>13</sup>C NMR (CDCl<sub>3</sub>)  $\delta$  212.0 (s), 172.7 (s), 138.0 (s), 136.5 (s), 129.5 (d), 128.7 (d), 128.4 (d), 128.0 (s), 127.7 (d), 127.3 (d), 126.7 (d), 123.2 (s), 62.8 (d), 62.1 (s), 44.9 (d), 44.6 (t), 43.8 (d), 41.7 (t), 39.0 (t), 36.2 (t), 33.2 (s), 30.7 (q), 29.6 (t), 23.1 (q), 19.8 (q), 16.1 (q). Anal. Found: C, 81.75; H, 8.12; N, 3.16. C<sub>30</sub>H<sub>35</sub>N<sub>2</sub>O<sub>2</sub> requires C, 81.59; H, 7.99; N, 3.17.

(24) The crystal structure of an earlier, racemic version of tricyclic compound **22** was determined by using standard procedures. Crystals of **22** belong to space group *P*2<sub>1</sub>*a* with *a* = 17.602, *b* = 15.312, and *c* = 9.486 Å and  $\beta = 97.62^\circ$ . The structure was solved by using the MULTAN program and refined to an *R* of 0.14, at which point refinement was terminated. A difference Fourier map revealed no peaks larger than 0.45 e/Å<sup>3</sup>. Figure 1 shows an ORTEP stereo plot of the structure of **22**.

(25) It seems quite likely that the bulky *N*-benzyl substituent is serving to destabilize nonreactive conformers in a manner similar to that found by Gschwend in his studies with *E*-amides (ref 5).

(26) Department of Chemistry.

(27) Department of Medicinal Chemistry and Pharmacognosy.

(28) Postdoctoral Research Associate.

(29) Graduate Research Associate.

(30) A. P. Sloan Fellow 1977-1979.

trometer and John Saddler for providing those spectra.

**Supplementary Material Available:** Listings of observed and calculated structural factors and bond lengths and bond angles (18 pages). Ordering information is given on any current masthead page.

Stephen G. Pyne,<sup>26,28</sup> Mark J. Hensel,<sup>26,29</sup> Stephen R. Byrn<sup>27</sup>  
Ann T. McKenzie,<sup>27</sup> P. L. Fuchs<sup>\*26,30</sup>

Departments of Chemistry and  
Medicinal Chemistry and Pharmacognosy  
Purdue University, West Lafayette, Indiana 47907

Received January 18, 1980

## Effect of Photoelectrode Crystal Structure on Output Stability of Cd(Se,Te)/Polysulfide Photoelectrochemical Cells

Sir:

Cadmium chalcogenides have received a great deal of attention as photoelectrodes in polychalcogenide redox couple containing photoelectrochemical cells since the stabilizing effect of these redox couples on them was discovered.<sup>1-3</sup> Most of the attention was focused on CdSe, for which *long-term* output stability in polysulfide solutions (with or without added Se) was achieved by using single crystals,<sup>4</sup> pressed pellets,<sup>5</sup> and electroplated<sup>1,6</sup> or painted<sup>7</sup> thin layers. Stabilization of the low-band-gap material CdTe ( $E_G = 1.45$  eV vs. 1.75 eV for CdSe, at room temperature) was achieved at low-output currents only, i.e., short-circuit currents below those expected at reasonable quantum efficiencies under solar illumination conditions.<sup>1,8,9</sup> Under such conditions, CdTe thin layers in polysulfide solution<sup>1,8,10</sup> and polytelluride solution<sup>1,8</sup> and single crystals in selenide or telluride solution<sup>9</sup> were stable at low photocurrent densities.

We report here on thin-film polycrystalline Cd(Se,Te) alloy photoelectrodes, which show output stability comparable to CdSe photoelectrodes<sup>6</sup> when possessing the hexagonal (wurtzite) structure and which have optical band gaps similar to that of pure CdTe.<sup>11</sup> CdSe and CdTe form homogeneous alloys over the whole composition range,<sup>11,12</sup> with the alloy adopting the cubic (sphalerite) or hexagonal (wurtzite) structure, depending on the composition and conditions of preparation. Figure 1 shows the variation of the optical band gap (absorption edge) of the alloys as a function of composition and crystal structure.<sup>11</sup> Similar behavior is observed for Cd(S,Te) alloys<sup>11,13</sup> while Cd(S,Se) alloys show monotonic dependence of their band gaps on composition.<sup>11</sup> The latter alloys have been used successfully as photoelectrodes in polysulfide solution.<sup>14</sup> Both the cubic and the hexagonal forms

(1) Hodes, G.; Manassen, J.; Cahen, D. *Nature (London)* **1976**, *261*, 403; *Bull. Isr. Phys. Soc.* **1976**, *22*, 100.

(2) Ellis, A. B.; Kaiser, S. W.; Wrighton, M. S. *J. Am. Chem. Soc.* **1976**, *98*, 1635; *Ibid.* **1976**, *98*, 6855.

(3) Miller, B.; Heller, A. *Nature (London)* **1976**, *262*, 680.

(4) Heller, A.; Schwartz, G. P.; Vadimsky, R. G.; Menezes, S.; Miller, B. *J. Electrochem. Soc.* **1978**, *125*, 1156.

(5) Miller, B.; Heller, A.; Robbins, M.; Menezes, S.; Chang, K. C.; Thomson, J., Jr. *J. Electrochem. Soc.* **1977**, *124*, 1019.

(6) Cahen, D.; Hodes, G.; Manassen, J. *J. Electrochem. Soc.* **1978**, *125*, 1623.

(7) Hodes, G.; Cahen, D.; Manassen, J.; David, M. *J. Electrochem. Soc.*, in press.

(8) Manassen, J.; Hodes, G.; Cahen, D. U.S. Patent 4064 326, 1977.

(9) Ellis, A. B.; Kaiser, S. W.; Bolts, J. M.; Wrighton, M. S. *J. Am. Chem. Soc.* **1977**, *99*, 2839; *Ibid.* **1976**, *98*, 6418.

(10) Danaher, W. J.; Lyons, L. E. *Nature (London)* **1978**, *271*, 139.

(11) Brodin, M. S.; Vitrikhovskii, N. I.; Kipen', A. A.; Mizetskaya, I. B. *Sov. Phys.-Semicond. (Engl. Transl.)* **1972**, *6*, 601; Tai, H.; Nakashima, S.; Hori, S. *Phys. Status Solidi. A* **1975**, *30*, K115.

(12) Stuckes, A. D.; Farrell, G. *J. Phys. Chem. Solids* **1964**, *25*, 477.

(13) Hill, R.; Casper, A. N. *Solid State Commun.* **1975**, *17*, 735; NSF RANN AER 75-15858 (International Workshop on CdS Solar Cells and Other Abrupt Heterojunctions, April 30-May 2, 1975, University of Delaware) **1975**, 265.

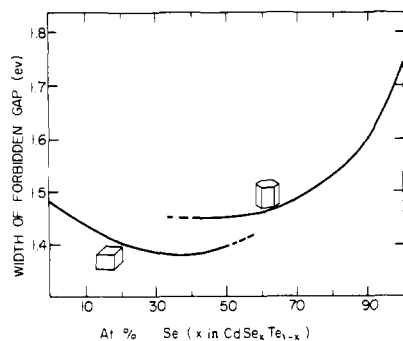


**Figure 1.** Variation of room temperature optical (direct) band gap of Cd(Se,Te) as a function of Se content and crystal structure for well-annealed samples (solid lines). Quenched samples, alloys prepared under pressure, or electroplated samples may adopt the opposite crystal modification, depending on conditions (dashed lines).

of Cd(Se,Te) roughly follow Vegard's law, i.e., show a linear dependence of their lattice dimensions on stoichiometry between the end members, pure CdSe and CdTe.<sup>12</sup> Under equilibrium conditions (well annealed, slowly cooled), there exists a range of stoichiometries where the cubic and hexagonal phases can coexist (Figure 1).

The preparation of thin polycrystalline films of the alloys, described in more detail elsewhere,<sup>7</sup> was essentially as follows. Measured amounts of CdSe and CdTe powders were mixed together with ~25% (w/w) of a suitable flux, e.g., CdCl<sub>2</sub>, and fired for ~40 min between 630 and 660 °C in an Ar atmosphere. The resulting material was ground up, washed free of excess flux, mixed with ~5–10% (w/w) flux, and mixed with a liquid (e.g., H<sub>2</sub>O containing ~5% nonionic detergent) to obtain a smooth slurry. This slurry was applied to a conducting substrate (e.g., slightly oxidized Ti metal) and annealed for 10–15 min in Ar containing 20 ppm of O<sub>2</sub> at ~650 °C. The resulting layers had a grain size of 10–30 μm and were ~20 μm thick.<sup>7</sup> The photoactivity of the resulting electrodes (in polysulfide) could be improved by a short etch in 3% HNO<sub>3</sub> in HCl and by dipping in concentrated aqueous K<sub>2</sub>CrO<sub>4</sub>. Electrodes (1 cm<sup>2</sup>) of CdSe<sub>0.65</sub>Te<sub>0.35</sub> gave open-circuit voltages up to 680 mV, short-circuit currents up to 15 mA, and fill factors of ~0.5, under illumination equal to 0.85 × AM1 for materials of this kind [ $\eta$ (solar) ~5%]. This performance could be improved further by purposely photocorroding the electrodes for a few seconds in dilute acid,<sup>15</sup> yielding improved short-circuit voltage currents ( $\geq 18$  mA) and fill factors ( $\geq 0.55$ ), and open-circuit voltages as before, and consequently solar conversion efficiencies of 7.5–8% (the highest reported so far for polycrystalline thin-film photoelectrochemical cells).<sup>16</sup> Photoresponse measurements showed an onset of photocurrent at ~930 nm and a linear, constant, response from 810 nm downward (~1.45-eV band gap) for electrodes with this composition.

All electrodes were investigated by X-ray powder diffraction and found to be mainly hexagonal when the Se content was higher than 60 atom % and mainly cubic when less Se was present. Table I gives the lattice dimensions for some of the electrodes.

Figure 2 shows the output stability of several electrodes. We observe a dramatic decrease in stability once the cubic phase<sup>18</sup> is the dominant one, at a given stoichiometry. Experiments with electrodes containing 60 atom % Se and 40 atom % Te, which were annealed for different periods, thus varying the amount of cubic phase present, showed that, also at a fixed stoichiometry, a decrease in stability is found when the cubic phase increases at the cost of the hexagonal phase (Figure 2 shows the 60:40

**Table I.** Crystallographic Data<sup>a</sup> for CdSe<sub>x</sub>Te<sub>1-x</sub>

composition	hexagonal			cubic <i>a</i> <sub>0</sub> , Å
	<i>x</i> <sup>b</sup>	% <sup>c</sup>	<i>a</i> , Å	
1.00	100	4.31	7.02	6.05 <sup>d</sup>
0.70	100	4.38	7.16	
0.65	>95	4.40	7.18	6.23
0.63	>90	4.42	7.20	6.24
0.60	70 (±10)	4.43	7.23	6.26
0.57	30 (±10)	4.44	7.24	6.27
0.55	<5	4.44	7.25	6.28
0.50	0			6.30
0.00	0	4.60 <sup>d</sup>	7.50 <sup>d</sup>	6.48

<sup>a</sup> From X-ray-powder-diffraction data of photoelectrodes.

<sup>b</sup> From relative amounts of starting materials. <sup>c</sup> As estimated from powder-diffraction patterns (see legend, Figure 2). <sup>d</sup> Literature data; for comparison only.

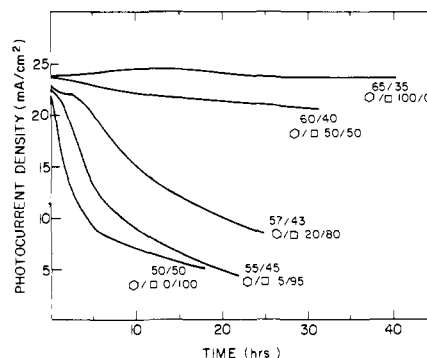


**Figure 2.** Output stability of several Cd(Se,Te) alloys in a solution 2 M each in KOH, Na<sub>2</sub>S·9H<sub>2</sub>O, and S at 35 °C. Potentiostatic short-circuit measurements were made with a Pt counterelectrode. Photoelectrode area: ~0.2 cm<sup>2</sup>; illumination intensity chosen so as to obtain identical initial photocurrent densities for all electrodes (±10% range of intensities). Light source: stabilized W-I<sub>2</sub> projector lamp. Stoichiometries (upper numbers) determined from relative amounts of parent materials used in preparation and verified by X-ray diffraction by using Vegard's law (see Table I). Estimates of percentage of cubic and hexagonal phases (lower numbers) based on comparison of X-ray diffraction peak intensities of (111) for cubic and (1010), (0002), and (1011) for hexagonal, as well as (004) for cubic and (1012) and (1013) reflections for hexagonal phase.<sup>17</sup>

composition with low hexagonal content annealed under the same conditions as the other examples in this figure).

This pronounced difference in output stability is rather surprising in view of the very close structural relation between the two phases. The hexagonal phase is essentially a close-packed ABAB hexagonal stacking of tetrahedrally coordinated Cd atoms while the cubic phase has ABCABC stacking, i.e., only the stacking arrangement differentiates between the two, with the immediate (first coordination shell) vicinity being identical in the two forms.

One possible reason for the different stabilities could be preferred orientation of the Cd(Se,Te) crystallites in the photoelectrodes, as the output stability of hexagonal CdSe, at least, is known to depend on the kind of crystal face exposed to the S<sub>x</sub><sup>2-</sup> solution, with exposure of the (1120) face resulting in higher stability than either the (0001) or the (1010) face<sup>4</sup> (G. Hodes, J. Manassen, and D. Cahen, to be published). Furthermore, the (1120) face is known to be a preferred cleavage plane of the wurtzite phase as is the crystallographically equivalent (110) face of the sphalerite phase.<sup>19</sup> However, no preferred orientation of these planes was found from a comparison of intensities of experimental X-ray-powder-diffraction patterns of Cd(Se,Te) with intensities calculated from the known crystal structure.<sup>20</sup>

(19) See, for example: Mason, B.; Berry, L. G. "Elements of Mineralogy", W. H. Freeman: San Francisco, 1968.

(20) These comparisons show preferred orientation of the (1010) plane in the wurtzite phase and of the, crystallographically similar, (111) plane in the sphalerite phase.

(14) Noufi, R. N.; Kohl, P. A.; Bard, A. J. *J. Electrochem. Soc.* **1978**, *125*, 376.

(15) Hodes, G. *Nature (London)* **1980**, *285*, 29.

(16) Heller, A.; Miller, B.; Chu, S. S.; Lee, Y. T. *J. Am. Chem. Soc.* **1979**, *101*, 7633.

(17) Hartmann, H. *Krist. Tech.* **1966**, *1*, 267.

(18) The name of this phase, sphalerite, after the ZnS mineral with this structure seems particularly appropriate for our experiments ( $\sigma\phi\alpha\lambda\epsilon\sigma = \text{perilous, slippery}$ ).

Therefore, it is rather unlikely that preferred orientation can explain the observed stability differences.

Another possibility is that the CdS layer, which is formed on the electrode in  $S_x^{2-}$  solution, will always have the hexagonal structure, which would cause a larger lattice mismatch with an underlying cubic phase than with a hexagonal one. Such a lattice mismatch would influence the "rate matching"<sup>6,21</sup> between hole flux and electrochemical reaction, and by it the ability of  $S^{2-}$  oxidation to prevent photoelectrode self-oxidation. However, preliminary experiments on cubic  $(CdTe)_{0.25}(ZnSe)_{0.75}$ , which show this phase to behave similar to hexagonal Cd(Se,Te) phases in terms of output stability, can be construed as evidence against this possibility.

The most likely explanation may be found in a difference in bond strengths between hexagonal and cubic Cd(Se,Te) of the same chemical composition. The lower band gap of the cubic form, as compared to the hexagonal one (with the same stoichiometry), can be associated with a weaker interaction between the Cd and the chalcogen, something that is expressed in the effective ionic charges on Cd. These charges are much smaller in cubic CdTe than in hexagonal CdS and CdSe.<sup>22</sup> Rough calculations on hexagonal ZnS, by using the method of ref 21, yield an effective ionic charge of  $\sim 0.4$ <sup>23</sup> while that for cubic ZnS is  $\sim 0.3$ <sup>22</sup> (ZnS was chosen because its piezoelectric coefficients are well-known for both phases). Extrapolating to Cd(Se,Te), we expect stronger bonding (higher heat of formation per bond according to Pauling's ionicity) in the hexagonal phase than in the cubic one. Since the stability of Cd chalcogenides in polysulfide solutions depends on the relative probabilities of self-oxidation (which requires breaking a Cd-chalcogen bond) and interfacial charge transfer, a small increase in bond strength can improve the semiconductor stability profoundly.<sup>24</sup>

This explanation of the observed differences in output stability implies that the decomposition potentials<sup>25,26</sup> for the two phases are different. In view of the results from ref 4, as well as our own, a further dependence of these potentials on the orientation of the exposed crystal face is likely as well. Experiments to clarify these points further are now in progress in this laboratory.<sup>27</sup>

(21) Cahen, D.; Manassen, J.; Hodes, G. *Sol. Energy Mater.* **1979**, *1*, 343.

(22) Berlincourt, D.; Jaffe, H.; Shiozawa, L. R. *Phys. Rev.* **1963**, *129*, 1009.

(23) Piezoelectric data from "Landolt-Bornstein Tables", Springer-Verlag: West Berlin, Vol. III/3, 1979.

(24) The difference in effective ionic charge may affect the electrochemical reaction rate as well. However, since the electrode surface is converted rapidly into CdS, especially once current starts flowing, such an effect is unlikely, unless the nature of the newly formed CdS depends on that of the underlying phase.

(25) Gerischer, H. J. *Electroanal. Chem.* **1977**, *82*, 133.

(26) Bard, A. J.; Wrighton, M. S. *J. Electrochem. Soc.* **1977**, *124*, 1706.

(27) Partial support by Ormat Turbines Ltd. and the U.S. Israel Binational Science Foundation, Jerusalem, Israel, is gratefully acknowledged.

Gary Hodes, Joost Manassen, David Cahen\*  
Weizmann Institute of Science  
Rehovot, Israel

Received March 28, 1980

## Biosynthesis of Antibiotics of the Virginiamycin Family. 1. Biosynthesis of Virginiamycin M<sub>1</sub>: Determination of the Labeling Pattern by the Use of Stable Isotope Techniques

Sir:

Virginiamycin M<sub>1</sub> (1) was first isolated from *Streptomyces virginiae*,<sup>1</sup> but the same compound has been isolated from a number of different microorganisms and has also been named as ostreogrycin A, mikamycin A, staphylomycin M<sub>1</sub>, pristinamycin

(1) Somer, P. de; Dijk, P. J. *Antibiot. Chemother. (Washington, D.C.)* **1955**, *5*, 632-639.

Table I. Incorporation of <sup>3</sup>H- and <sup>14</sup>C-Labeled Presursors into Virginiamycin M<sub>1</sub>

precursor added	% incorporation
sodium [2- <sup>14</sup> C] acetate	5.0
L-[methyl- <sup>3</sup> H] methionine	4.0
DL-[3- <sup>14</sup> C] serine	1.4
L-[3,4- <sup>3</sup> H <sub>2</sub> ] proline	5.0
D-[U- <sup>14</sup> C] glucose	0.6
[2- <sup>14</sup> C] glycine	0.4, 0.8 <sup>a</sup>
L-[U- <sup>14</sup> C] alanine	b

<sup>a</sup> Data from ref 13. <sup>b</sup> No measurable incorporation (ref 13).

IIA, streptogramin A, and PA 114 Al.<sup>2,3</sup> Its structure was originally determined by a combination of chemical and instrumental techniques<sup>4,5</sup> and has been confirmed by X-ray crystallography.<sup>6</sup>

The antibiotic is of interest from a biosynthetic viewpoint because it contains the unusual dehydroproline and oxazole ring systems. Although the origin of dehydroamino acids has been discussed previously,<sup>7,8</sup> the only experimental evidence bearing on the formation of the oxazole ring is found in work on the biosynthesis of the alkaloid annuloline<sup>9</sup> and in recent work on the biosynthesis of berninamycin, where it was postulated that <sup>14</sup>C-labeled serine and threonine were both incorporated into the oxazole units of this antibiotic.<sup>10</sup> In this communication, we report results which establish the overall biosynthetic origin of the major portion of virginiamycin M<sub>1</sub>, including the oxazole ring.

Virginiamycin M<sub>1</sub> was produced in baffled 250-mL Erlenmeyer flasks containing 30 mL of a complex nutrient broth.<sup>11</sup> These were inoculated with a culture of *S. virginiae* strain PDT-30 and shaken at 21 °C. After 1 day, labeled precursors were added, and the broths were worked up 1 day later. Virginiamycin M<sub>1</sub> was isolated by extraction of the broth with hexane followed by ethyl acetate, and purification of the crude ethyl acetate extract by high-performance liquid chromatography.<sup>12</sup> Incorporation of radioactive precursors was determined by counting the chromatographically homogeneous product; this procedure was checked in one instance by addition of authentic antibiotic and recrystallization to constant specific activity.

Table I lists the <sup>3</sup>H- and <sup>14</sup>C-labeled precursors fed and the percent incorporation of each. These results broadly corroborate those reported earlier for incorporation of various <sup>14</sup>C-labeled substrates into virginiamycin.<sup>13</sup>

Feeding experiments with [2-<sup>13</sup>C]acetate, [1,2-<sup>13</sup>C<sub>2</sub>]acetate, L-[methyl-<sup>13</sup>C]methionine, and DL-[3-<sup>13</sup>C]serine gave <sup>13</sup>C-labeled antibiotic in yields of 10-20 mg/L, and materials thus obtained were analyzed by <sup>13</sup>C NMR spectroscopy. The natural-abundance proton-noise-decoupled <sup>13</sup>C NMR spectrum of virginiamycin M<sub>1</sub> shows signals for 28 carbon atoms. Assignment of the relevant signals was made by using characteristic chemical shifts, multiplicities, single-frequency proton decoupling, and analysis of one-bond carbon-carbon couplings in pairs of carbon atoms; our

(2) Crooy, P.; Neys, R. *de J. Antibiot.* **1972**, *25*, 371-372.

(3) Cocito, C. *Microbiol. Rev.* **1979**, *145*-198.

(4) Delpierre, G. R.; Eastwood, F. W.; Gream, G. E.; Kingston, D. G. I.; Todd, A. R.; Williams, D. H. *J. Chem. Soc. C* **1966**, 1653-1669.

(5) Kingston, D. G. I.; Todd, A. R.; Williams, D. H. *J. Chem. Soc. C* **1966**, 1669-1676.

(6) Durant, F.; Evrard, G.; Declercq, J. P.; Germain, G. *Cryst. Struct. Commun.* **1974**, *3*, 503-510.

(7) Bycroft, B. W. *Nature (London)* **1969**, *224*, 595-597.

(8) Schmidt, V.; Häusler, J.; Öhler, E.; Poisel, H. *Fortschr. Chem. Org. Naturst.* **1979**, *37*, 251-327.

(9) O'Donovan, D. G.; Horan, H. *J. Chem. Soc. C* **1971**, 331-334.

(10) (a) Pearce, C. J.; Rinehart, K. L., Jr. *J. Am. Chem. Soc.* **1979**, *101*, 5069-5070. (b) Rinehart, K. L., Jr.; Weller, D. D.; Pearce, C. J. *J. Nat. Prod.* **1980**, *43*, 1-20.

(11) The broth, designated STA-14, contained the following components (amount expressed as g/L): corn steep solids (20), peanut oil cake (10), yeast autolyzate (5), glucose (5), glycerol (25), linseed oil (10), calcium carbonate (5).

(12) Kingston, D. G. I. *J. Nat. Prod.* **1979**, *42*, 237-260.

(13) Roberfroid, M.; Dumont, P. *Ind. Chim. Belge* **1967**, *32*, 307-309.